Water Induced Structural Transformations in Flexible 2D Layered Conductive Metal–Organic Frameworks

Yuliang Shi, Mohammad R. Momeni*, Yen-Jui Chen, Zeyu Zhang, and Farnaz A. Shakib*

Department of Chemistry and Environmental Science, New Jersey Institute of Technology, Newark 07102, NJ United States

E-mail: shakib@njit.edu,momeni@njit.edu

Contents

S1. Developing *ab initio* force fields **4**

Figure S1 5

Table S1 6

Table S2 7

Table S3 7

Table S4 8

Table S5 9

Table S6 10

Table S7 11

Table S8 11

Table S9 12

Table S10 13

S2. Validation of the developed force fields **14**

Figure S2 15

Figure S3 16

Figure S4 17

Figure S5 18

Figure S6 18

S2. Cluster electronic structure calculations **19**

S3. Details of MD simulation **20**

Figure S7 20

Figure S8 21

S4. Structural dynamics of dry 2D MOFs Cu_3(HHTP)$_2$ and Co_3(HHTP)$_2$ **23**

Figure S9 24

Figure S10 25
Table S11 26
Figure S11 27
Figure S12 28
Figure S13 29
Figure S14 30
Figure S15 30
Table S12 31
Table S13 32
Table S14 33
Table S15 34
Table S16 35
Table S17 36
Table S18 37
Table S19 38
Table S20 39
Table S21 40
Table S22 41
Figure S16 42
Figure S17 43

References **44**

S1. Developing *ab initio* force fields

Optimized structures of 2D MOFs at 0 K using conventional *static* electronic structure methods are too perfect for reflecting the flexible nature of these layered materials. Here, we study 2D MOFs via our developed flexible *ab initio* force fields (AIFFs) that allows deformation of both layers and the unit cell, providing a realistic picture of the structural and dynamical properties of 2D MOFs. We started from the experimental crystallographic data available for aqueous $Co_3(HHTP)_2$[1] to build a 2×2×2 super cell for the dry MOF by removing hydrolyzed layers, solvent molecules and all chemisorbed water molecules, and then adjusting the interlayer distances to ∼4 Å. This supercell was optimized with periodic boundary conditions. Both cell vectors and atomic positions were minimized using the PBE[2] density functional with damped D3 dispersion correction[3] in CP2K version 5.1.[4] Generic force fields such as generalized amber force field (GAFF)[5] were never developed for systems with transition metals and hence the force field parameters for them do not exist. In this work, we used the David Carrol's genetic algorithm[6] for fitting all interactions involving the Co^{2+} and Cu^{2+} transition metal centers including bonds, angles, and dihedrals while all parameters involving the intramolecular interactions present in the organic linkers were taken from GAFF without further modification. For creating a training set, reduced cluster models comprised of a single Co/Cu center and two catecholate linkers were cut from the optimized crystal structures, Figure S1.

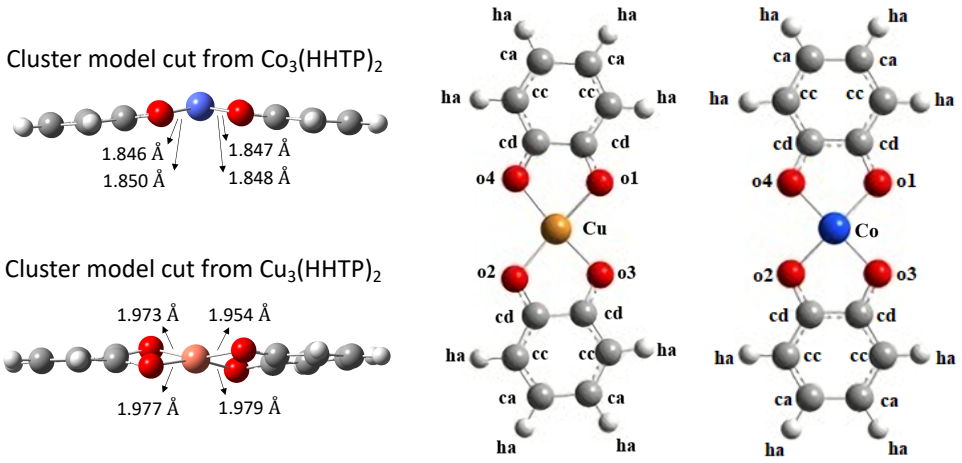

Figure S1: Left: side view of cluster models cut from the optimized 2×2 crystal structure to build the training set. Middle and right: top view of the same cluster models with the atom labels used in developing *ab initio* force fields for $Cu_3(HHTP)_2$ and $Co_3(HHTP)_2$ 2D MOFs.

The linking carbon ends of the benzene rings were kept frozen to mimic the integrity of the framework. The central metal atoms were then displaced by 0.02 Å from -0.04 Å to +0.04 Å along the x, y and z dimensions (creating a total of 125 configurations). All electronic energies for this training set were then calculated using the ωB97M-v[7] density functional and the Def2-TZVP basis set as implemented in QCHEM 5.2.[8] To fit force field parameters to this *ab initio* training set, Morse potential was used for all coordinative metal-oxo bonds which allows investigating the possibility of hydrolysis and differentiating properties of $Cu_3(HHTP)_2$ and $Co_3(HHTP)_2$ in presence of confined water. Harmonic potential was employed for the rest. Atomic charges were computed at the ωB97X-D/Def2-TZVP level[7] using the CHELPG scheme which fits all atomic charges to represent molecular electrostatic potential.[9] The complete list of the bonded and non-bonded parameters for $Cu_3(HHTP)_2$ and $Co_3(HHTP)_2$ MOFs are given in Tables S1-S5 and S6-S10, respectively. The Lennard-Jones parameters for Cu are taken from the Universal Force Field (UFF)[10] while the parameters for Co are adapted from a recent study.[11]

Table S1: Electrostatic and Lennard-Jones non-bonded parameters for $Cu_3(HHTP)_2$ MOF where r_{ij} refers to the distance between two atoms.

$$V_{LJ}(r) = 4\epsilon\Big[\Big(\frac{\sigma}{r_{ij}}\Big)^{12} - \Big(\frac{\sigma}{r_{ij}}\Big)^{6}\Big] \tag{1}$$

Atom name	Atom type	Charge	ε (kcal·mol^{-1})	σ / 2 (Å)
Cu	Cu	1.2399	0.27600	1.14500
o1	o1	-0.6004	0.17000	1.50001
o2	o2	-0.6794	0.17000	1.50001
o3	o3	-0.6495	0.17000	1.50001
o4	o4	-0.6242	0.17000	1.50001
cd	C	0.3795	0.08600	1.69983
cc	C	-0.1251	0.08600	1.69983
ca	C	-0.0889	0.08600	1.69983
ha	H	0.1629	0.01500	1.29982

Table S2: Harmonic bond potential parameters for $Cu_3(HHTP)_2$ MOF.

$$V_{bond}(r) = \frac{1}{2}K_{ij}(r_{ij} - r_0)^2 \tag{2}$$

Bond type (Harmonic)	K_{ij}(kcal mol^{-1}Å^{-2})	r_0(Å)
ca-cc	770.200012	1.456000
ca-ca	922.200012	1.398000
ca-ha	691.599976	1.086000
cd-o1	1039.400000	1.275000
cc-ha	698.200012	1.084000
cc-cd	1001.799988	1.373000
cd-o2	1039.400000	1.275000
cd-cd	839.599976	1.428000
cd-o3	1039.400000	1.275000
cd-o4	1039.400000	1.275000

Table S3: Morse bond potential parameters for $Cu_3(HHTP)_2$ MOF.

$$V_{Morse}(r) = E_0[(1 - e^{-K_{ij}(r_{ij}-r_0)})^2 - 1] \tag{3}$$

Bond type (Morse)	E_0(kcal mol^{-1})	r_0(Å)	K_{ij}(Å^{-1})
Cu-o1	377.652433	2.000318	0.796643
Cu-o2	345.598932	2.039822	0.408112
Cu-o3	276.258160	2.016915	1.158078
Cu-o4	545.175119	1.970611	0.517874

Table S4: Bending potential parameters for $Cu_3(HHTP)_2$ MOF.

$$V_{angle}(\theta) = \frac{1}{2} K_{ijk}(\theta_{ijk} - \theta_0)^2 \tag{4}$$

Angle type (Harmonic)	K_{ijk}(kcal mol^{-1}deg^{-2})	$\theta(^\circ)$
o1-Cu-o2	290.461154	165.213724
o3-Cu-o4	283.944477	163.001614
o2-Cu-o4	236.467396	101.611571
o1-Cu-o3	212.535810	94.999561
o1-Cu-o4	285.623947	86.636287
o2-Cu-o3	193.430370	85.440569
Cu-o2-cd	210.382777	107.723868
Cu-o1-cd	132.416365	105.103340
Cu-o4-cd	198.251713	105.036526
Cu-o3-cd	57.652500	110.267558
ca-cc-ha	91.599998	124.000000
ca-cc-cd	135.199997	113.500000
ca-ca-cc	130.000000	120.699997
ca-ca-ha	96.400002	119.800003
cd-cd-o1	139.000000	117.300003
cc-cd-o1	140.199997	120.300003
cc-ca-ha	96.400002	119.800003
cc-cd-o2	140.199997	120.300003
cc-cd-cd	136.399994	114.099998
cd-cc-ha	97.000000	121.699997
cd-cd-o3	139.000000	117.300003
cd-cd-o4	139.000000	117.300003
cd-cd-o2	139.000000	117.300003
cc-cd-o3	140.199997	120.300003
cc-cd-o4	140.199997	120.300003

Table S5: Torsion potential parameters for $Cu_3(HHTP)_2$ MOF.

$$V_{torsion}(\phi) = K_{ijkl}[1 + \cos(m\phi_{ijkl} - \delta)] \quad (5)$$

Dihedral type (Cosine)	K_{ijkl}(kcal mol^{-1})	$\delta(^\circ)$	m
o1-Cu-o2-cd	5.559125	180.0000	2
o1-Cu-o3-cd	7.027488	180.0000	2
o1-Cu-o4-cd	6.090330	180.0000	2
cc-cd-o2-Cu	1.972223	180.0000	2
o3-Cu-o2-cd	4.430417	180.0000	2
o4-Cu-o2-cd	2.147997	180.0000	2
cd-cd-o3-Cu	1.783663	180.0000	2
o2-Cu-o1-cd	4.343647	180.0000	2
o3-Cu-o1-cd	2.495295	180.0000	2
o4-Cu-o1-cd	0.367073	180.0000	2
cd-cd-o4-Cu	1.928278	180.0000	2
o2-Cu-o3-cd	2.000299	180.0000	2
o2-Cu-o4-cd	6.967154	180.0000	2
cc-cd-o3-Cu	3.132602	180.0000	2
o3-Cu-o4-cd	2.641955	180.0000	2
cc-cd-o4-Cu	0.127274	180.0000	2
cd-cd-o1-Cu	1.607713	180.0000	2
cd-cd-o2-Cu	1.385652	180.0000	2
o4-Cu-o3-cd	3.495792	180.0000	2
cc-cd-o1-Cu	0.235726	180.0000	2
ca-cc-cd-o2	12.0000	180.0000	2
ca-cc-cd-cd	12.0000	180.0000	2
ca-ca-cc-ha	5.6000	180.0000	2
ca-ca-cc-cd	5.6000	180.0000	2
cc-cd-cd-o1	12.0000	180.0000	2
o1-cd-cd-o4	12.0000	180.0000	2
ca-cc-cd-o1	12.0000	180.0000	2
ha-cc-cd-o1	12.0000	180.0000	2
cc-ca-ca-cc	9.0000	180.0000	2
cc-ca-ca-ha	9.0000	180.0000	2
cc-cd-cd-cc	12.0000	180.0000	2
cc-cd-cd-o3	12.0000	180.0000	2
ha-ca-cc-ha	5.6000	180.0000	2
ha-cc-cd-o2	12.0000	180.0000	2
ha-cc-cd-cd	12.0000	180.0000	2
ha-ca-cc-cd	5.6000	180.0000	2
cc-cd-cd-o2	12.0000	180.0000	2
o2-cd-cd-o3	12.0000	180.0000	2
ca-cc-cd-o3	12.0000	180.0000	2
ha-cc-cd-o3	12.0000	180.0000	2
ca-cc-cd-o4	12.0000	180.0000	2
ha-cc-cd-o4	12.0000	180.0000	2
cc-cd-cd-o4	12.0000	180.0000	2
ha-ca-ca-ha	9.0000	180.0000	2

Table S6: Electrostatic and Lennard-Jones non-bonded parameters for $Co_3(HHTP)_2$ MOF.

Atom name	Atom type	Charge	ε (kcal·mol^{-1})	σ / 2 (Å)
Co	Co	1.3869	0.00150	1.08420
o1	o1	-0.6685	0.17000	1.50001
o2	o2	-0.6339	0.17000	1.50001
o3	o3	-0.6538	0.17000	1.50001
o4	o4	-0.6335	0.17000	1.50001
cd	C	0.3285	0.08600	1.69983
cc	C	-0.1236	0.08600	1.69983
ca	C	-0.0880	0.08600	1.69983
ha	H	0.1838	0.01500	1.29982

Table S7: Harmonic bond potential parameters for $Co_3(HHTP)_2$ MOF.

Bond type (Harmonic)	K_{ij}(kcal mol^{-1}Å^{-2})	r_0(Å)
ca-cc	770.200012	1.456000
ca-ca	922.200012	1.398000
ca-ha	691.599976	1.086000
cd-o1	1039.400000	1.275000
cc-ha	698.200012	1.084000
cc-cd	1001.799988	1.373000
cd-o2	1039.400000	1.275000
cd-cd	839.599976	1.428000
cd-o3	1039.400000	1.275000
cd-o4	1039.400000	1.275000

Table S8: Morse bond potential parameters for $Co_3(HHTP)_2$ MOF.

Bond type (Morse)	E_0(kcal mol^{-1})	r_0(Å)	K_{ij}(Å^{-1})
Co-o1	746.686742	1.854732	0.930179
Co-o2	465.241494	1.833957	1.651822
Co-o3	512.186873	1.846134	0.846275
Co-o4	141.677562	1.856311	1.423639

Table S9: Bending potential parameters for $Co_3(HHTP)_2$ MOF.

Angle type (Harmonic)	K_{ijk}(kcal mol^{-1}deg^{-2})	$\theta(^\circ)$
o1-Co-o2	23.826317	166.417418
o1-Co-o3	158.509367	169.211587
o1-Co-o4	57.929895	91.432950
Co-o2-cd	143.818954	88.837165
Co-o1-cd	90.726710	82.909712
o2-Co-o3	18.416613	81.717877
o2-Co-o4	116.582600	116.028227
o3-Co-o4	1.322023	110.645184
Co-o4-cd	91.242458	116.814723
Co-o3-cd	133.802770	117.834518
ca-cc-ha	91.599998	124.000000
ca-cc-cd	135.199997	113.500000
ca-ca-cc	130.000000	120.699997
ca-ca-ha	96.400002	119.800003
cd-cd-o1	139.000000	117.300003
cc-cd-o1	140.199997	120.300003
cc-ca-ha	96.400002	119.800003
cc-cd-o2	140.199997	120.300003
cc-cd-cd	136.399994	114.099998
cd-cc-ha	97.000000	121.699997
cd-cd-o3	139.000000	117.300003
cd-cd-o4	139.000000	117.300003
cd-cd-o2	139.000000	117.300003
cc-cd-o3	140.199997	120.300003
cc-cd-o4	140.199997	120.300003

Table S10: Torsion potential parameters for $Co_3(HHTP)_2$ MOF.

Dihedral type (Cosine)	K_{ijkl}(kcal mol^{-1})	$\delta(^\circ)$	m
o1-Co-o2-cd	4.983060	180.000000	2
o1-Co-o3-cd	1.524057	180.000000	2
o1-Co-o4-cd	7.189605	180.000000	2
cc-cd-o2-Co	6.673697	180.000000	2
o3-Co-o2-cd	6.848685	180.000000	2
o4-Co-o2-cd	6.814635	180.000000	2
cd-cd-o3-Co	5.590086	180.000000	2
o2-Co-o1-cd	4.873418	180.000000	2
o3-Co-o1-cd	3.710804	180.000000	2
o4-Co-o1-cd	4.710728	180.000000	2
cd-cd-o4-Co	7.355621	180.000000	2
o2-Co-o3-cd	0.711884	180.000000	2
o2-Co-o4-cd	7.264709	180.000000	2
cc-cd-o3-Co	4.070400	180.000000	2
o3-Co-o4-cd	5.603407	180.000000	2
cc-cd-o4-Co	5.882635	180.000000	2
cd-cd-o1-Co	5.327184	180.000000	2
cd-cd-o2-Co	7.816238	180.000000	2
o4-Co-o3-cd	6.591315	180.000000	2
cc-cd-o1-Co	6.577384	180.000000	2
ca-cc-cd-o2	12.0000	180.0000	2
ca-cc-cd-cd	12.0000	180.0000	2
ca-ca-cc-ha	5.6000	180.0000	2
ca-ca-cc-cd	5.6000	180.0000	2
cc-cd-cd-o1	12.0000	180.0000	2
o1-cd-cd-o4	12.0000	180.0000	2
ca-cc-cd-o1	12.0000	180.0000	2
ha-cc-cd-o1	12.0000	180.0000	2
cc-ca-ca-cc	9.0000	180.0000	2
cc-ca-ca-ha	9.0000	180.0000	2
cc-cd-cd-cc	12.0000	180.0000	2
cc-cd-cd-o3	12.0000	180.0000	2
ha-ca-cc-ha	5.6000	180.0000	2
ha-cc-cd-o2	12.0000	180.0000	2
ha-cc-cd-cd	12.0000	180.0000	2
ha-ca-cc-cd	5.6000	180.0000	2
cc-cd-cd-o2	12.0000	180.0000	2
o2-cd-cd-o3	12.0000	180.0000	2
ca-cc-cd-o3	12.0000	180.0000	2
ha-cc-cd-o3	12.0000	180.0000	2
ca-cc-cd-o4	12.0000	180.0000	2
ha-cc-cd-o4	12.0000	180.0000	2
cc-cd-cd-o4	12.0000	180.0000	2
ha-ca-ca-ha	9.0000	180.0000	2

S2. Validation of the developed force fields

The developed force fields are validated against available experimental data. The interlayer distances obtained from our MD simulations were compared to the experimentally measured powder X-ray diffraction data as shown in Figure S2 below. For the simulated spectra shown in Figure S2 the final MD equilibrated systems as shown and discussed in the main text were employed. The first four prominent peaks in the simulated PXRDs indicate the long-range order within the ab plane, in good agreement with the experimental PXRD reported in Ref. 12 and Ref. 1 for both MOFs (though the forth peak is almost nonexistent in the experimental PXRD of $Co_3(HHTP)_2$). Additionally, weaker and broader peaks at $2\theta = 24.4^\circ$ and $24.8^\circ$for $Cu_3(HHTP)_2$ and $Co_3(HHTP)_2$, respectively, corresponding to the [001] reflections, are indicative of poorer long-range order along the c direction, as expected for van der Waals linked layered materials. Similar [001] peaks for experimental PXRDs are observed at slightly higher values of 2θ as been the case for previous studies in comparison between simulated and experimental PXRDs, e.g. see Figure S2 of the SI of Ref. 12. We have used Bragg's equation ($\lambda = 2d\sin(\theta)$) to calculate the interlayer distance from these broad peaks resulting in $d = 0.364$ and $d = 0.358$ nm, for $Cu_3(HHTP)_2$ and $Co_3(HHTP)_2$, respectively which are in good agreement with the same calculation on experimental PXRD resulting in $d = 0.316$ and $d = 0.322$ nm, respectively.

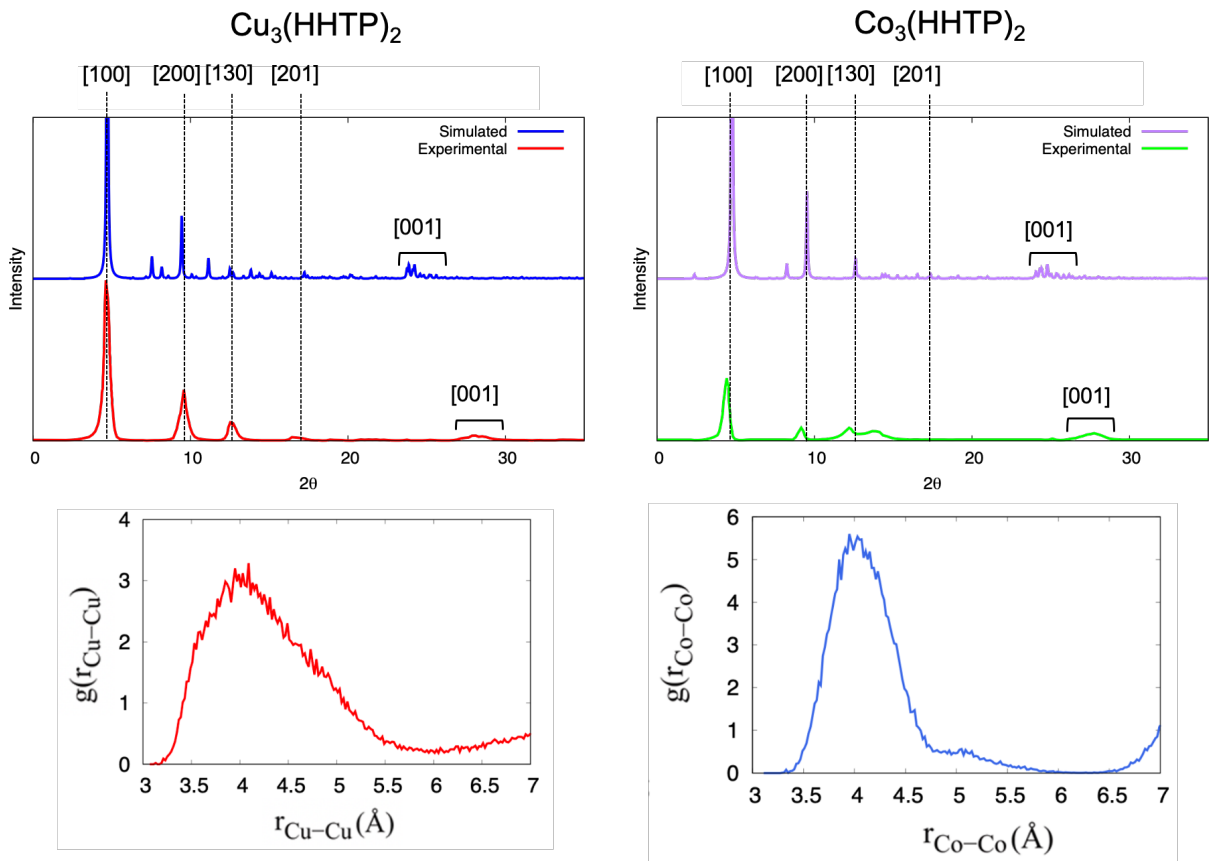

Figure S2: (a) Experimental and simulated (with using our MD equilibrated systems) powder X-Ray diffraction patterns for $Cu_3(HHTP)_2$ (left) and $Co_3(HHTP)_2$ (right) 2D MOFs. Experimental data are adapted from the SI of Ref. 12 which are in agreement with the previously reported PXRD data.[1]

The calculated radial distribution function (RDF) of Cu-Cu distances shows a prominent broad peak centered at ∼4 Å which indicates constant breathing of the stacked layers in the z direction. The equilibrated dry framework shows interlayer distances as small as 3 Å , see Figure S9b. However, deformation of flexible linkers leads to local instances of the increase of interlayer distances which would return to a shorter value afterwards, creating a constant breathing of layers. Similar breathing motion of layers is also characterized for $Co_3(HHTP)_2$ which shows interlayer distances as small as 3 Å , see Figure S10b, with a broad RDF peak centered at ∼4 Å.

To test the reliability of the developed force fields, we monitor the distribution of metal-oxo bond lengths at a wide range of temperatures from 93 K to 693 K at intervals of 100 K.

Normal distribution of bond lengths around the corresponding *ab initio* values confirm the stability of the developed force fields, Figure S3.

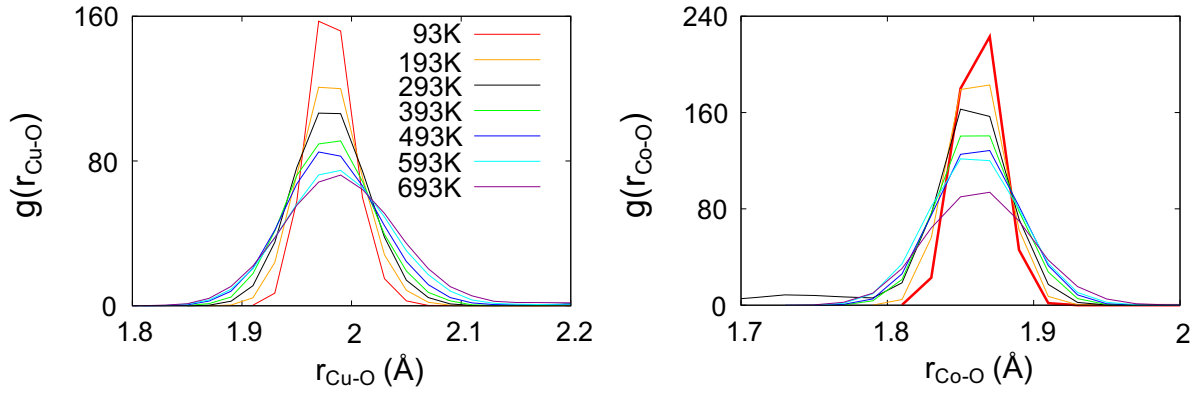

Figure S3: Distribution of representative metal-oxo bond lengths, Cu-o1 and Co-o1 of the $Cu_3(HHTP)_2$ and $Co_3(HHTP)_2$ 2D MOFs at temperatures ranging from 93 K to 693 K.

Further validation of the developed force fields come from comparison of force field Morse potentials to the *ab initio* energies with respect to the change of metal-oxo bond length.

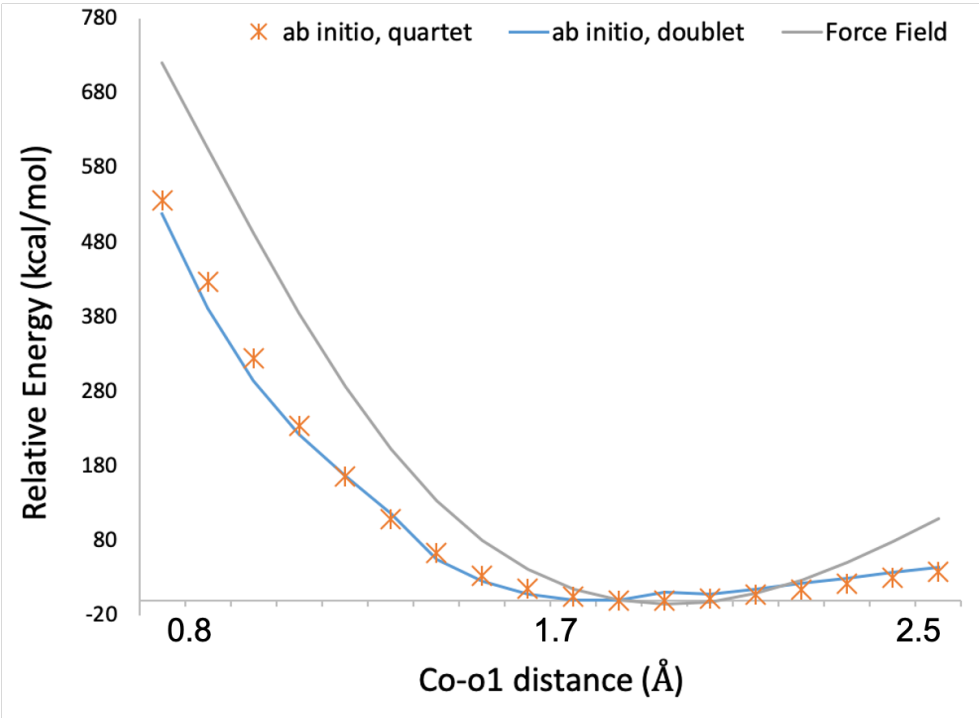

Figure S4: Comparison of our force field and reference *ab initio* energies at the ωB97M-v/def2-TZVP level for both the doublet and quartet spin states of the Co^{2+} cluster model shown in Figure S1. To obtain these correlation plots, the Co-o1 bond is scanned from 0.75 Å to 2.55 Å.

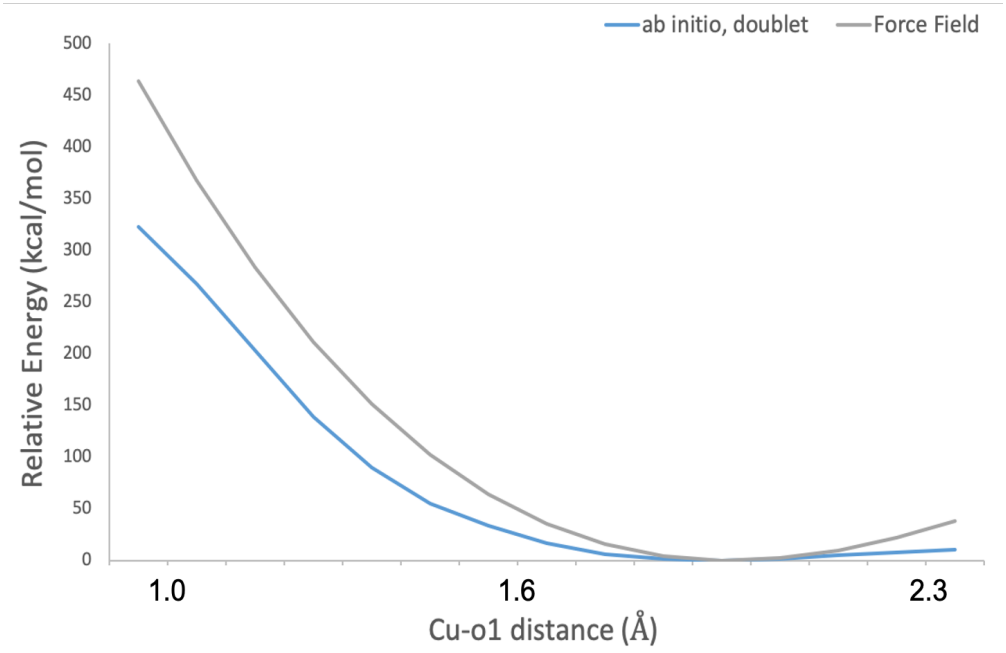

Figure S5: Comparison of our force field and reference *ab initio* energies at the ωB97M-v/def2-TZVP level for the doublet spin state of the Cu^{2+} cluster model shown in Figure S1. To obtain these correlation plots, the Cu-o1 bond is scanned from 0.95 Å to 2.35 Å.

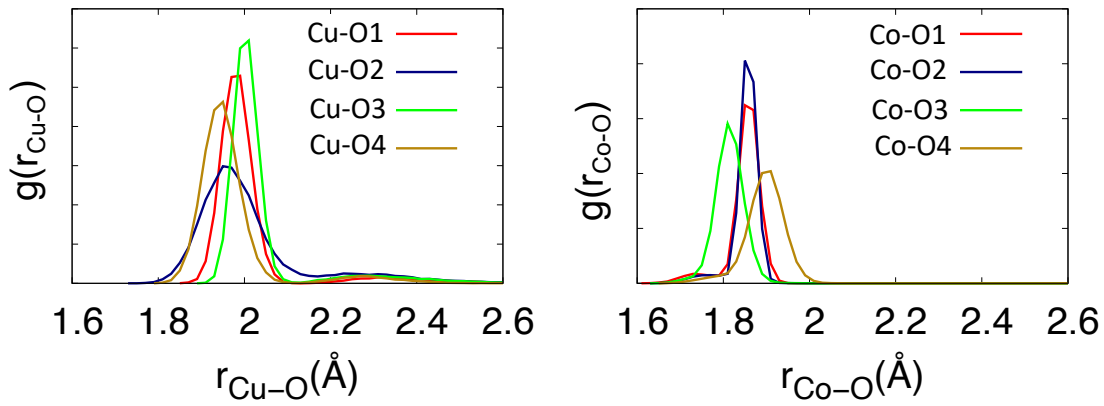

Figure S6: Calculated metal-oxo RDFs of the dry $Cu_3(HHTP)_2$ and $Co_3(HHTP)_2$ 2D MOFs at 293 K and 1 atm.

S3. Cluster electronic structure calculations

Cluster models were cut from their corresponding optimized 2×2×2 super cells with truncating the triphenylene organic linkers around the metal-oxo nodes to catecholate (Cartesian coordinates of all optimized structures are included as part of the Supporting Information (SI)). To transfer the rigidity of the MOF to the clusters, all the terminal carbon atoms of the benzene linkers were fixed to their positions in the optimized crystal structures. All cluster computations were carried out with Gaussian 16,[14] Revision A.03, where the meta-GGA local M06-L[15] density functional was used for all geometry optimizations and frequency calculations in gas phase using the Def2-SVP[16] basis set. Default convergence criteria was used for geometry optimizations which includes SCF=TIGHT (SCF convergence set to 10^{-8} Hartree) and "ultrafine grid" which requests a pruned (99,590) grid for the numerical integration of the two-electron integrals and their derivatives was used. This setting is especially recommended for molecules with soft low-frequency vibrational modes such as the ones studied in this work. The natures of all stationary points were determined by calculation of analytic vibrational frequencies, which were also used to compute molecular partition functions (298 K, 1 atm) using the conventional particle-in-a-box, rigid-rotator, quantum mechanical harmonic oscillator approximation,[17] except that all vibrational frequencies below 50 cm^{-1} were replaced with values of 50 cm^{-1} (the quasi-harmonic-oscillator approximation[17]). Zero imaginary vibrational frequency was found for all studied systems. Zero-point vibrational energies and thermal contributions to enthalpy were determined from these partition functions. Electronic energies were further refined by performing single point calculations with the ωB97M-v[7] density functional and the Def2-TZVP basis set as implemented in QCHEM 5.2.[8] The default convergence criterion for the SCF calculations which is 10^{-5} Hartree was used. All reported free energies and enthalpies are computed by combining ωB97M-v/def2-TZVP single point energies with thermochemical contributions obtained at the M06-L/def2-SVP level in gas phase.

S4. Details of MD simulation

Classical MD simulations for dry MOFs were performed on the hexagonal ($\alpha = \beta = 90°$, $\gamma = 120°$, $a = b = 46.470$ Å, and $c = 13.555$ Å) PBE-D3 minimized tetra-layered 2×2×2 supercell of the bulk $Co_3(HHTP)_2$ and $Cu_3(HHTP)_2$ MOFs (comprised of 1008 atoms in total and 48 metal centers) using DL_POLY_2 package.[18] Each system was equilibrated for 1 ns in the isothermal-isobaric NPT ensemble with a time step of 0.2 fs at 293 K temperature and 1 atm pressure, the experimental conditions at which the $Co_3(HHTP)_2$ crystals were synthesized,[1] allowing the simulation box to vary. To ensure that the systems were equilibrated for calculation of thermodynamical properties, longer simulations were run up to 7 ns. The constant total energy of the systems, with less than 1 kcal/mol fluctuation (Figure S2), confirms that 1 ns is enough for the dry MOFs to reach an equilibrated stage.

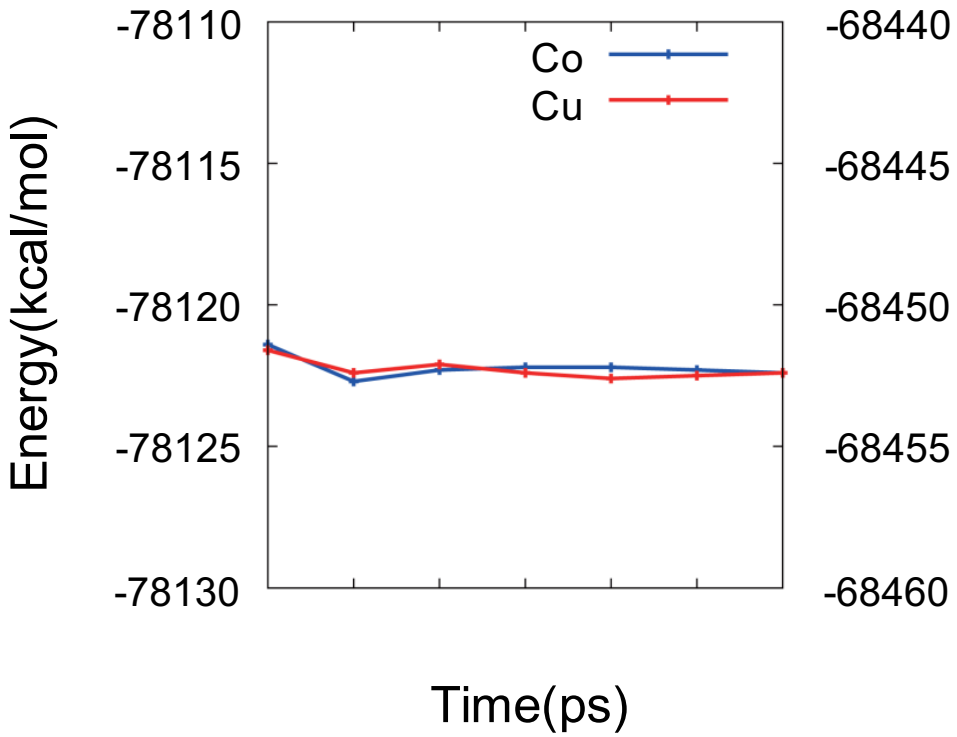

Figure S7: The total energy changes of dry $Cu_3(HHTP)_2$ in red and $Co_3(HHTP)_2$ in blue at 293K and 1 atm up to 7 ns in the NPT ensemble. The scale on the left-hand side shows the energies of Cu3(HHTP)2 while the right-hand side shows the energies of Co3(HHTP)2.

We also tested the convergence of total energy for the largest hydrated system, i.e. with added 192 water molecules inside the 1D channels. Simulations up to 9 ns shows that we need at least a 7 ns simulation run to reach an equilibrated stage. Hence, all water-contained systems were equilibrated for 7 ns in the isothermal-isobaric NPT ensemble with a time step of 0.2 fs. In each 1D channel of our 2×2×2 supercells, there are $n = 24$ open metal sites that are exposed to confined water molecules. Therefore, to study dynamics of confined water, we placed $n = 24$, $2n = 48$, $4n = 96$, $6n = 144$, and $8n = 192$ water molecules in a sphere centered at the middle of the 1D channel of the dry MOF using the PACKMOL[19] code. The simulations were carried out at 293 K temperature and 1 atm pressure.

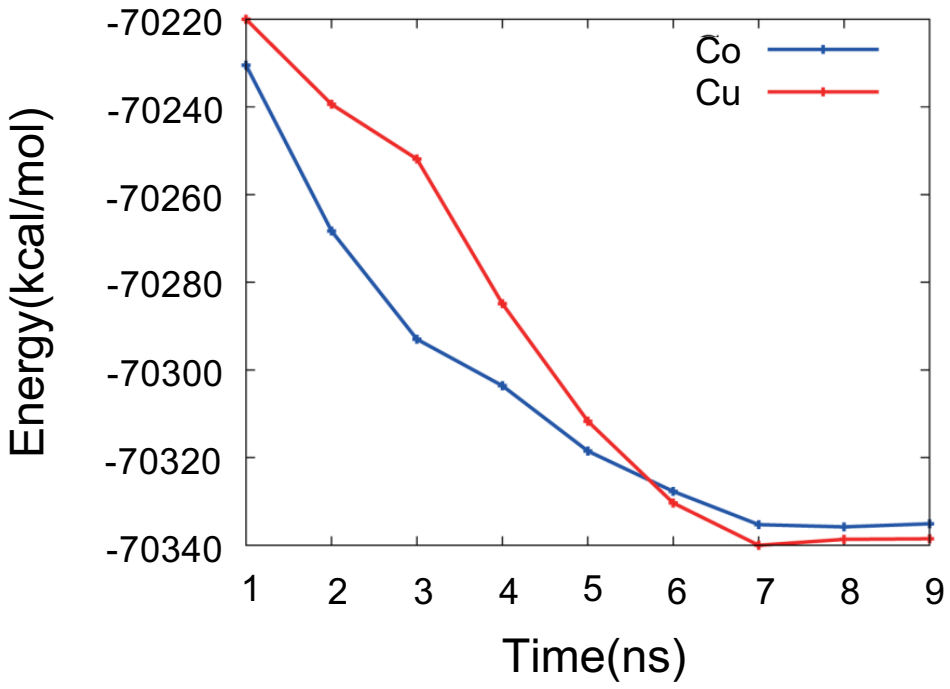

Figure S8: The total energy changes of 192@MOF for $Cu_3(HHTP)_2$ in red and $Co_3(HHTP)_2$ in blue up to 9 ns in the NPT ensemble.

The equations of motion were propagated according to the velocity-Verlet algorithm. The temperature was kept constant using a Nosé-Hoover chain comprised of four thermostats.[20] An atom-atom distance of 6.0 Å was employed for truncating the short-range interactions and the electrostatics were calculated using the Ewald summation method.[21] To account for

errors due to the truncation at 6.0 Å, long-range electrostatic interactions as implemented in DL_POLY_2 were applied to Lennard-Jones potentials. Lorentz-Berthelot mixing rules were used to drive cross interactions terms between water and the framework using the TIP4P/2005[22] water model. To model water molecules, we use the flexible 4-site qTIP4P/F[23] quantum water potential. The qTIP4P/F water model has been shown to be successful in reproducing a diverse number of static and dynamical properties of water including melting point, diffusion coefficients and IR spectrum. The implementation of qTIP4P/F model to DL_POLY_2 was carried out based on publicly available potentials distributed under the terms of the GNU General Public License at http://www.gnu.org/licenses/.[24] Dynamical properties are calculated from the average of 10 independent 50 ps NVE simulations. These trajectories were run from 10 different initial configurations obtained from a 10 ps NVT trajectory that followed the NPT simulations. The final snapshots of these NVT trajectories were then used as initial configurations for 50 ps NVE simulations ensuring that different starting configurations initiate independent NVE trajectories.

S5. Structural dynamics of the dry $Cu_3(HHTP)_2$ and $Co_3(HHTP)_2$ 2D MOFs

Figures S9a and S9b clearly show the slipping movement of the layers compared to each other and deformation of the organic linkers leading to rippled layers in $Cu_3(HHTP)_2$. Figures S10a and S10b show similar movements for $Co_3(HHTP)_2$. The prominent peak of Cu–O and Co–O RDFs in Figures S9c and S10c are related to coordinative metal-oxo bonds in one layer. Still, one can find small RDF peaks at higher distances which again emphasizes the slipping and breathing movements of the layers which bring the metal center of one layer closer to the oxygen atom of another layer. In fact, it is the combination of these movements that lead to formation of *intrinsic deformation sites* in $Co_3(HHTP)_2$. Figures S9d and S10d show long range order along the z direction, evidence of a π-stacked layer structure, through repeating Cu–Cu and Co–Co RDF peaks. Very noticeable broadening of the Cu–Cu RDF peak in Figure S9d compared to a narrow Co–Co RDF peak in Figure S10d shows more vivid breathing movement in $Cu_3(HHTP)_2$ compared to $Co_3(HHTP)_2$. This is indeed responsible for the fact that $Cu_3(HHTP)_2$ does not show *intrinsic deformation sites* at 293 K.

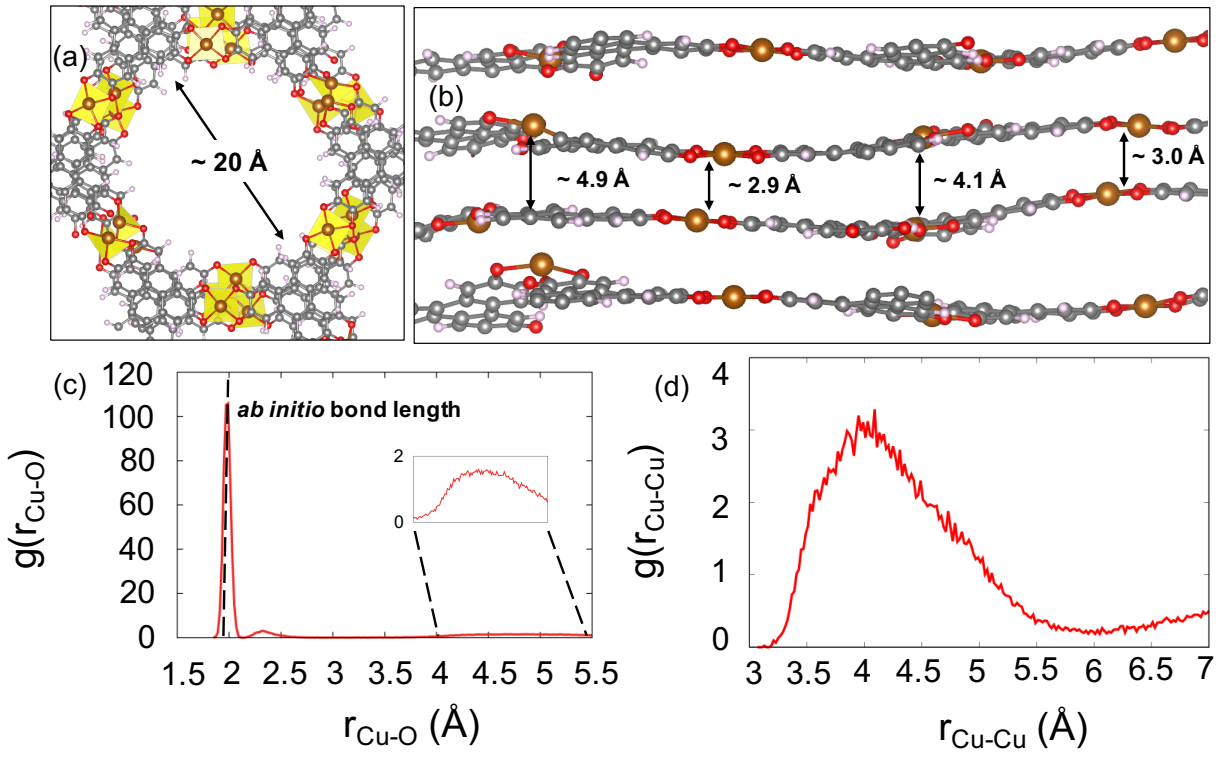

Figure S9: Rippling, slipping and breathing movements of the layers are evident in (a) top view, in z direction, and (b) side view, in xy plane, of the equilibrated structure of $Cu_3(HHTP)_2$ at 293 K. Copper is shown in brown and with tetrahedrons, oxygen in red, carbon in gray and hydrogen in pink. (c) and (d) demonstrate the radial distribution functions of Cu-O and Cu-Cu distances. For comparison, the computed Cu-O *ab initio* bond distance is highlighted with a black dash line.

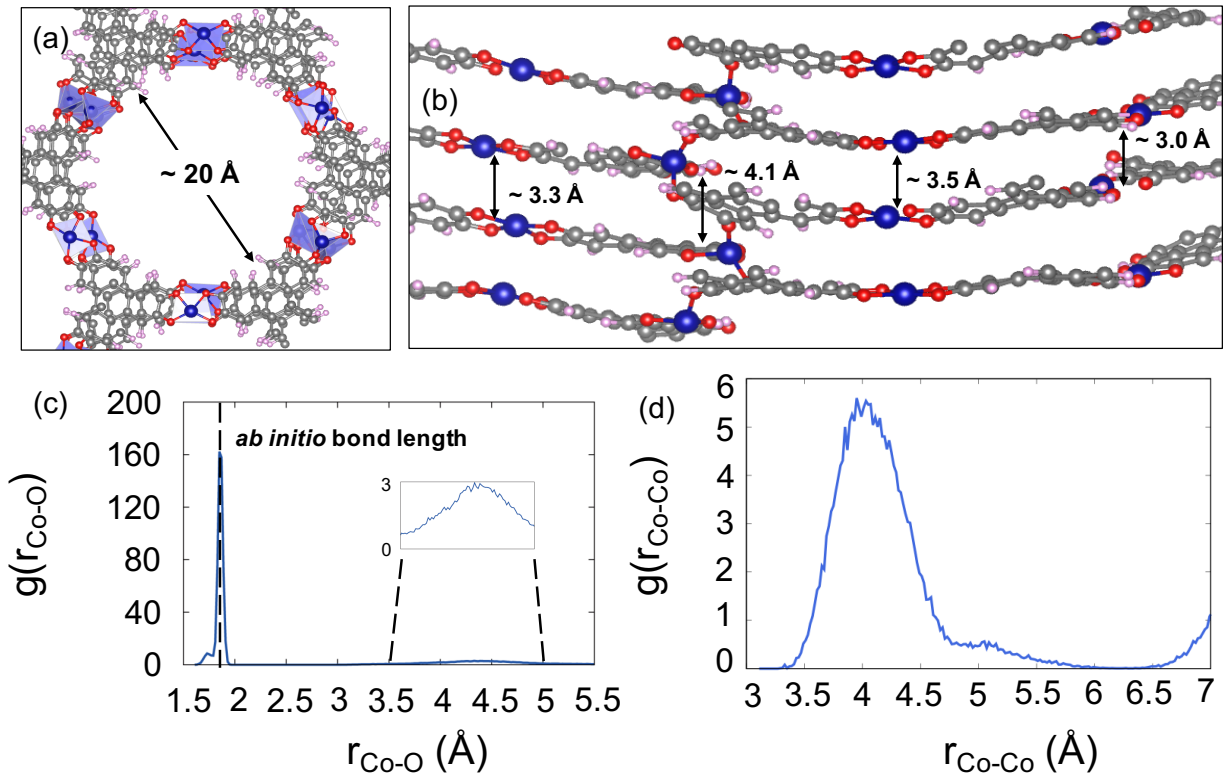

Figure S10: Rippling, slipping and breathing movements of the layers are evident in (a) top view, in z direction, and (b) side view, in xy plane, of the equilibrated structure of $Co_3(HHTP)_2$ at 293 K. Cobalt is shown in dark blue and with tetrahedrons, oxygen in red, carbon in gray and hydrogen in pink. (c) and (d) demonstrate the radial distribution functions of Co–O and Co–Co distances. For comparison, the computed Co-O *ab initio* bond distance is highlighted with a black dash line.

Table S11: Calculated PBE-D3(BJ)/DZVP-MOLOPT RESP charges for two different Co sites present in the $Co_3(HHTP)_2$ 2D MOF, (a) near planar Co sites and (b) tetrahedral *intrinsic deformation sites.*

Atom number	Charge	Atom number	Charge	Atom number	Charge
Sites (a)					
Co_{31}	+0.761	Co_{327}	+0.672	Co_{651}	+0.713
Co_{32}	+0.733	Co_{378}	+0.725	Co_{699}	+0.786
Co_{63}	+0.761	Co_{379}	+0.769	Co_{712}	+0.681
Co_{75}	+0.729	Co_{390}	+0.670	Co_{739}	+0.692
Co_{126}	+0.735	Co_{441}	+0.683	Co_{789}	+0.661
Co_{127}	+0.715	Co_{443}	+0.727	Co_{790}	+0.743
Co_{138}	+0.793	Co_{474}	+0.675	Co_{825}	+0.811
Co_{189}	+0.776	Co_{537}	+0.701	Co_{840}	+0.715
Co_{191}	+0.690	Co_{538}	+0.710	Co_{888}	+0.704
Co_{222}	+0.728	Co_{573}	+0.717	Co_{889}	+0.725
Co_{283}	+0.735	Co_{588}	+0.773	Co_{903}	+0.678
Co_{284}	+0.703	Co_{636}	+0.778	Co_{951}	+0.737
Co_{315}	+0.724	Co_{637}	+0.733	Co_{964}	+0.704
Co_{991}	+0.741				
Sites (b)					
Co_{64}	+0.997				
Co_{316}	+1.027				
Co_{574}	+0.974				
Co_{826}	+1.000				
Co_{190}	+1.091				
Co_{442}	+0.971				
Co_{700}	+0.867				
Co_{952}	+0.984				

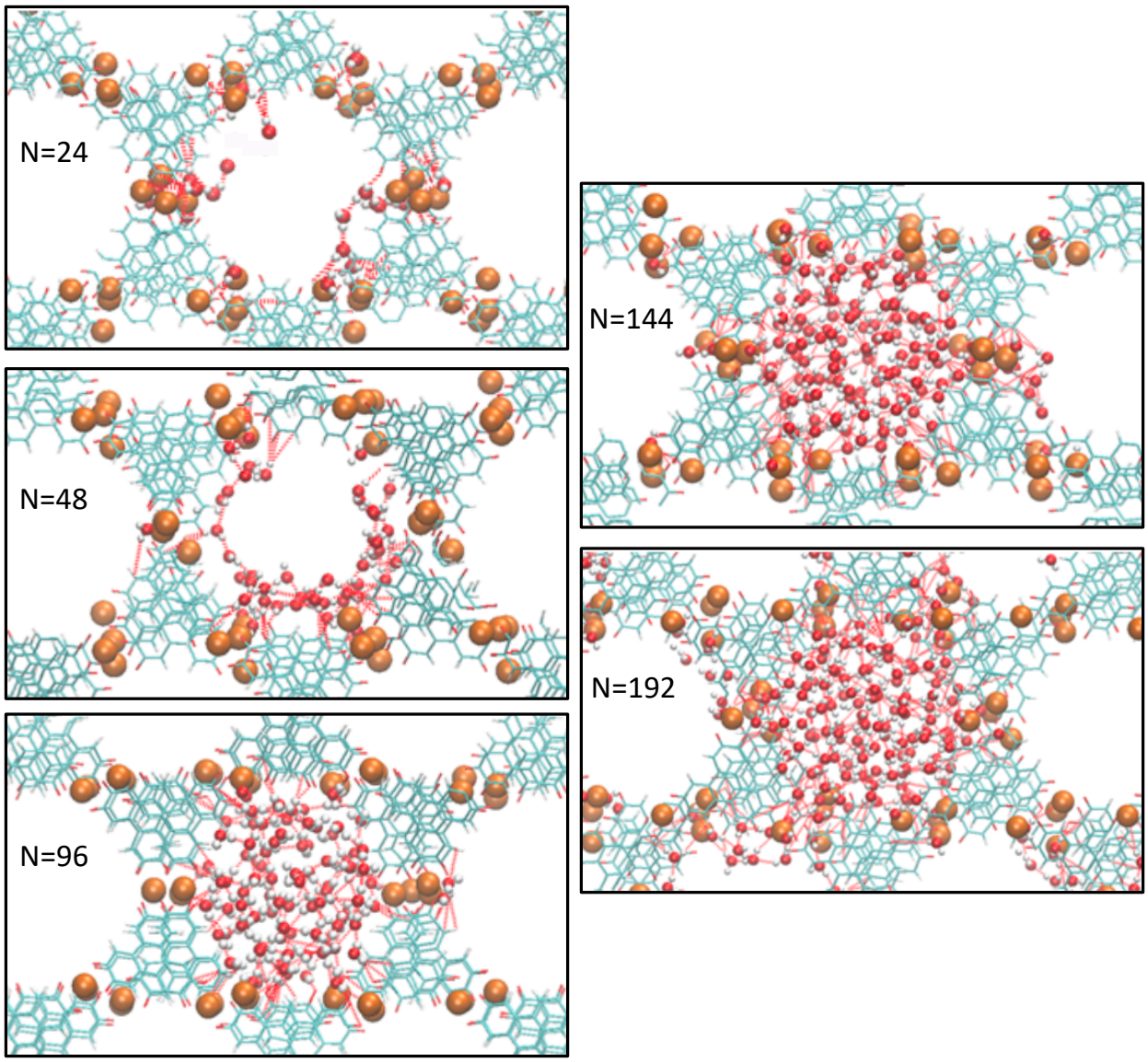

Figure S11: Top view of the hydrated $Cu_3(HHTP)_2$ systems with different water loadings. Diffusion of water molecules to the nearby channels in N=144 and 192 water molecules is evident. Also, the diffused water molecules prefer to stay adsorbed on the surface of the nearby channels rather than gathering at the center of the 1D channel.

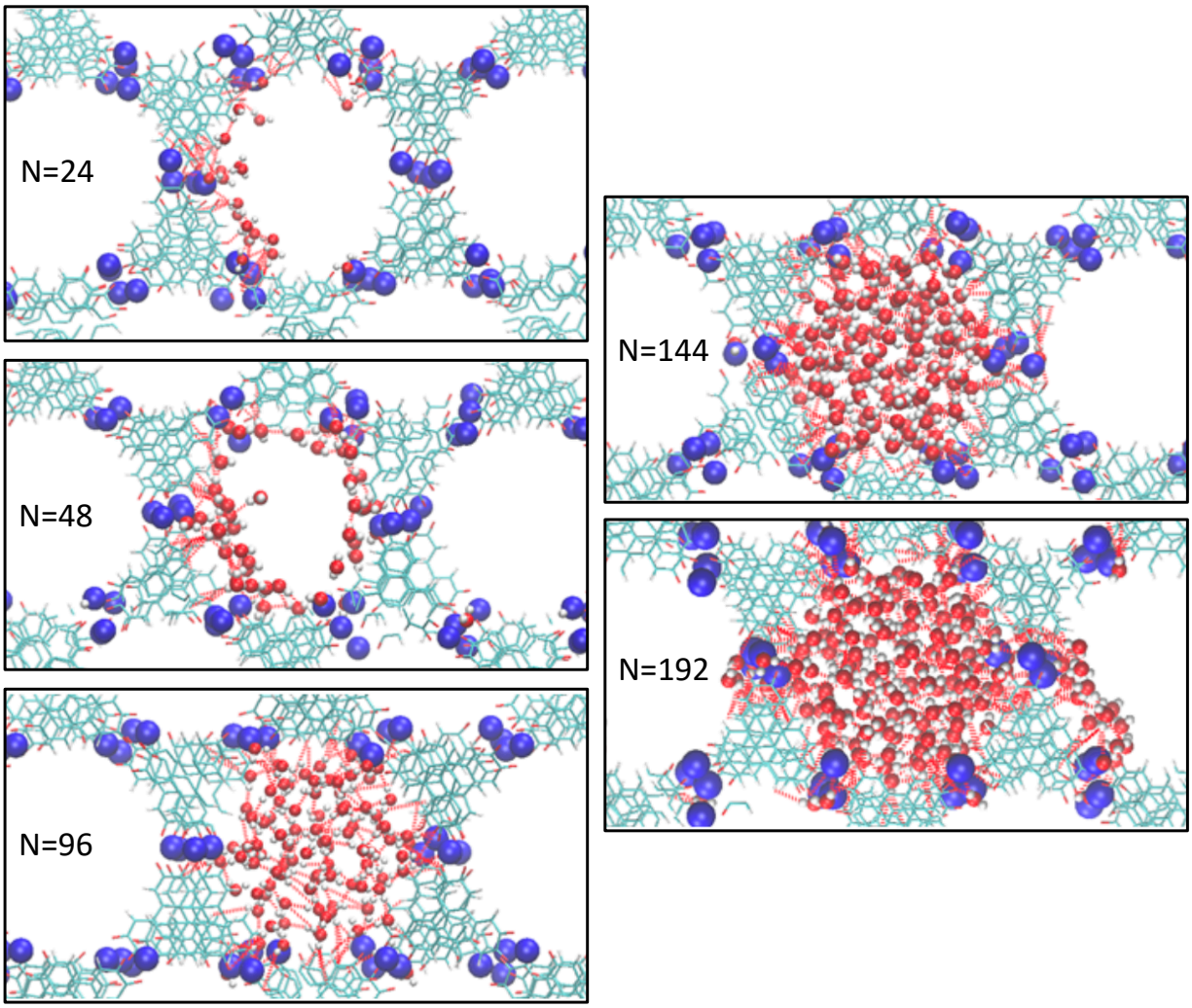

Figure S12: Top view of the hydrated $Co_3(HHTP)_2$ systems with different water loadings. Diffusion of water molecules to the nearby channels in N=144 and 192 water molecules is evident. Also, similar to the Cu system, the diffused water molecules prefer to stay adsorbed on the surface of the nearby channels rather than gathering at the center of the 1D channel.

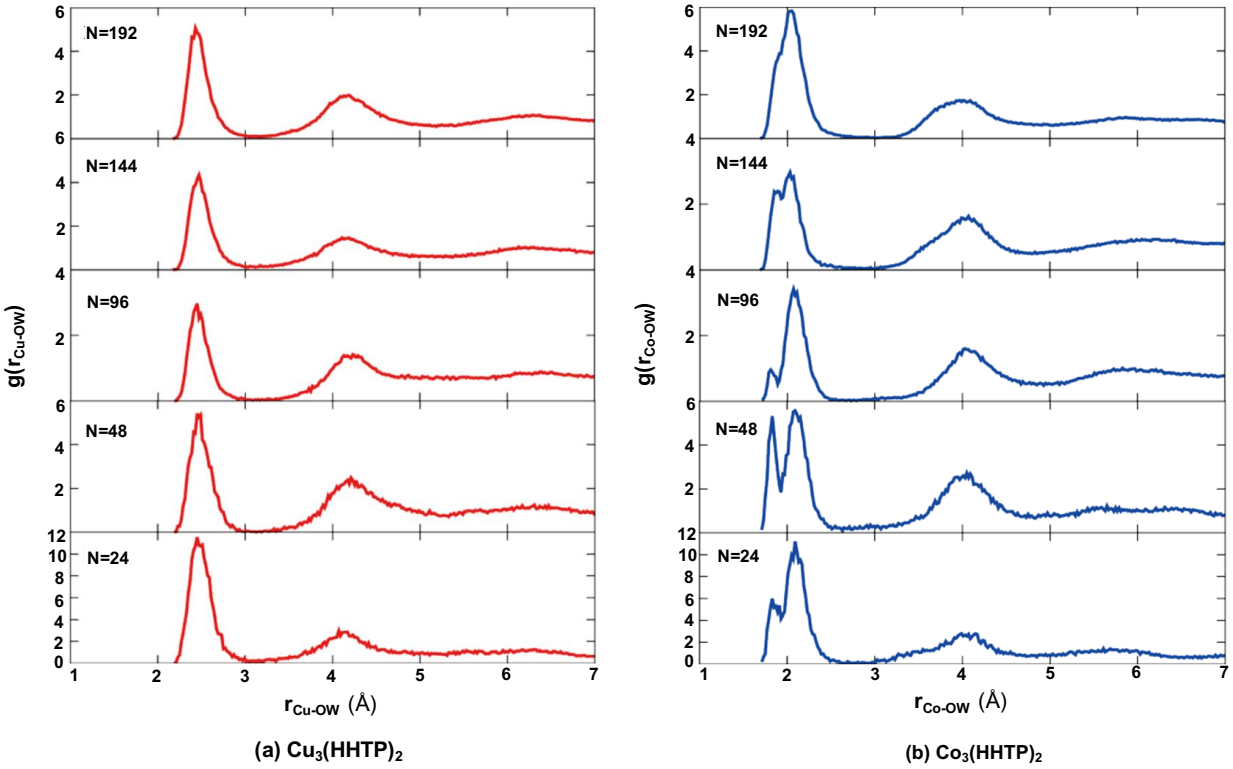

Figure S13: Calculated M-O_W (oxygen of water) RDFs for (a) $Cu_3(HHTP)_2$ and (b) $Co_3(HHTP)_2$ 2D MOFs with different water loadings.

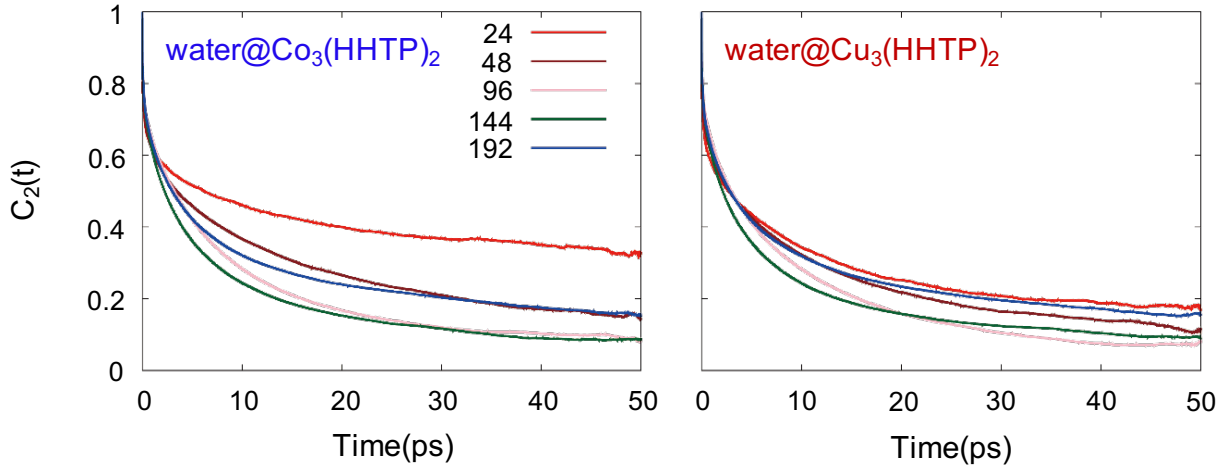

Figure S14: Orientational time correlation functions of the $Co_3(HHTP)_2$ and $Cu_3(HHTP)_2$ 2D MOFs with different water loadings.

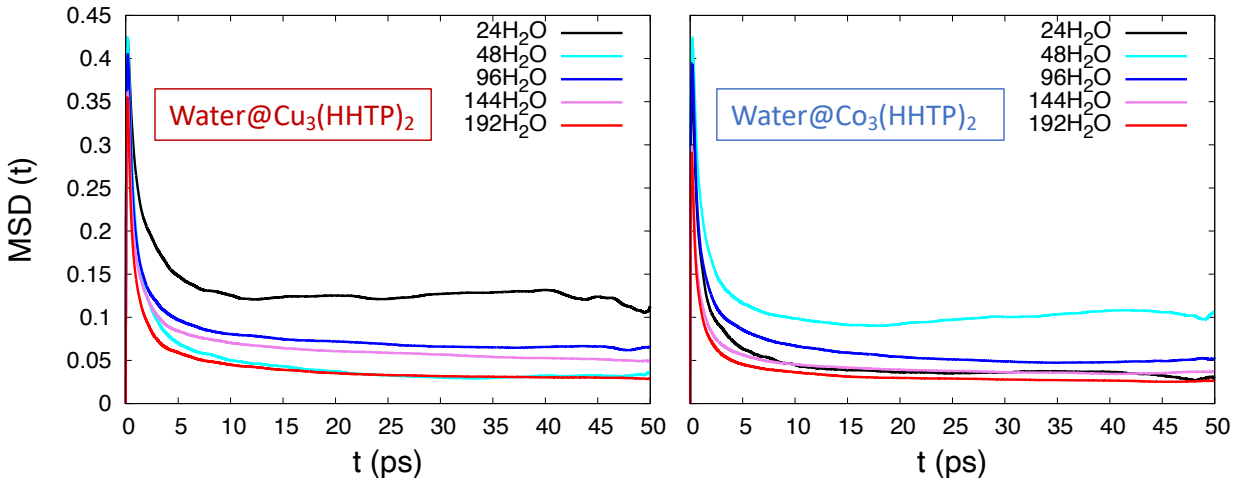

Figure S15: Mean Square Displacement (MSD) plots for the $Co_3(HHTP)_2$ and $Cu_3(HHTP)_2$ 2D MOFs with different water loadings obtained from 50 ps NVE simulations.

Table S12: Total diffusion coefficients (D_{tot}) in $Å^2 \cdot ps^{-1}$ and diffusion coefficients along the xy plane (D_{xy}) between the layers and z direction (D_z) along the 1D channels for $Cu_3(HHTP)_2$ and $Co_3(HHTP)_2$ MOFs with different water loadings.

	$Cu_3(HHTP)_2$			$Co_3(HHTP)_2$		
n	D_{tot}	D_{xy}	D_z	D_{tot}	D_{xy}	D_z
24	0.058±0.003	0.044±0.003	0.085±0.004	0.027±0.002	0.021±0.002	0.038±0.003
48	0.057±0.003	0.045±0.003	0.079±0.004	0.046±0.003	0.038±0.003	0.063±0.004
96	0.055±0.003	0.050±0.003	0.064±0.004	0.056±0.003	0.050±0.003	0.067±0.003
144	0.051±0.003	0.047±0.003	0.060±0.003	0.038±0.002	0.034±0.002	0.046±0.002
192	0.042±0.003	0.038±0.003	0.051±0.003	0.033±0.002	0.028±0.002	0.040±0.002

Table S13: Average simulation temperature for each of the 10 trajectories for $Co_3(HHTP)_2$ with 24 water molecules. Also listed is the average temperature over all 10 trajectories.

Trajectory	Average temperature(K)
1	292.955
2	288.978
3	291.722
4	268.175
5	296.779
6	295.735
7	290.246
8	292.977
9	295.824
10	295.658
Average	290.9049

Table S14: Average simulation temperature for each of the 10 trajectories for $Co_3(HHTP)_2$ with 48 water molecules. Also listed is the average temperature over all 10 trajectories.

Trajectory	Average temperature(K)
1	288.806
2	296.376
3	298.402
4	295.072
5	291.726
6	295.577
7	292.647
8	295.113
9	287.244
10	297.529
Average	293.8492

Table S15: Average simulation temperature for each of the 10 trajectories for $Co_3(HHTP)_2$ with 96 water molecules. Also listed is the average temperature over all 10 trajectories.

Trajectory	Average temperature(K)
1	288.54
2	295.13
3	295.707
4	290.811
5	293.529
6	296.039
7	234.361
8	297.001
9	291.983
10	295.174
Average	287.8275

Table S16: Average simulation temperature for each of the 10 trajectories for $Co_3(HHTP)_2$ with 144 water molecules. Also listed is the average temperature over all 10 trajectories.

Trajectory	Average temperature(K)
1	289.94
2	296.233
3	293.467
4	294.894
5	293.653
6	297.962
7	291.437
8	288.295
9	295.127
10	295.826
Average	293.6834

Table S17: Average simulation temperature for each of the 10 trajectories for $Co_3(HHTP)_2$ with 192 water molecules. Also listed is the average temperature over all 10 trajectories.

Trajectory	Average temperature(K)
1	291.996
2	292.496
3	288.604
4	289.456
5	294.146
6	291.78
7	295.423
8	292.896
9	289.511
10	289.03
Average	291.5338

Table S18: Average simulation temperature for each of the 10 trajectories for $Cu_3(HHTP)_2$ with 24 water molecules. Also listed is the average temperature over all 10 trajectories.

Trajectory	Average temperature(K)
1	292.918
2	301.27
3	290.835
4	294.365
5	286.786
6	294.246
7	291.158
8	290.248
9	291.733
10	293.189
Average	292.6748

Table S19: Average simulation temperature for each of the 10 trajectories for $Cu_3(HHTP)_2$ with 48 water molecules. Also listed is the average temperature over all 10 trajectories.

Trajectory	Average temperature(K)
1	288.78
2	297
3	292.84
4	296.933
5	302.098
6	286.101
7	293.061
8	296.094
9	295.337
10	286.77
Average	293.5014

Table S20: Average simulation temperature for each of the 10 trajectories for $Cu_3(HHTP)_2$ with 96 water molecules. Also listed is the average temperature over all 10 trajectories.

Trajectory	Average temperature(K)
1	292.651
2	294.621
3	296.6
4	295.791
5	291.388
6	289.766
7	293.708
8	299.271
9	290.857
10	293.859
Average	293.8512

Table S21: Average simulation temperature for each of the 10 trajectories for $Cu_3(HHTP)_2$ with 144 water molecules. Also listed is the average temperature over all 10 trajectories.

Trajectory	Average temperature(K)
1	290.222
2	293.351
3	297.934
4	293.174
5	295.154
6	297.965
7	295.323
8	289.494
9	298.432
10	293.178
Average	294.4227

Table S22: Average simulation temperature for each of the 10 trajectories for $Cu_3(HHTP)_2$ with 192 water molecules. Also listed is the average temperature over all 10 trajectories.

Trajectory	Average temperature(K)
1	293.346
2	296.212
3	294.718
4	294.3
5	292.945
6	293.587
7	294.451
8	291.011
9	296.73
10	293.512
Average	294.0812

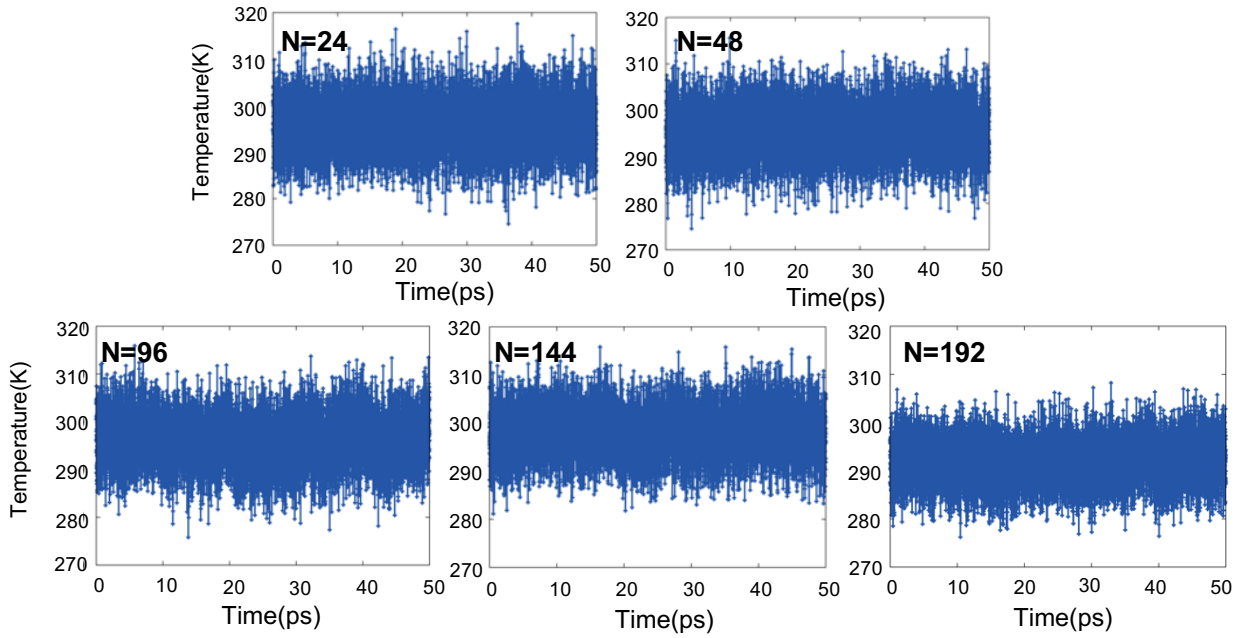

Figure S16: Simulation Temperature of the 6th NVE trajectory for different water content in the $Co_3(HHTP)_2$ 2D MOF.

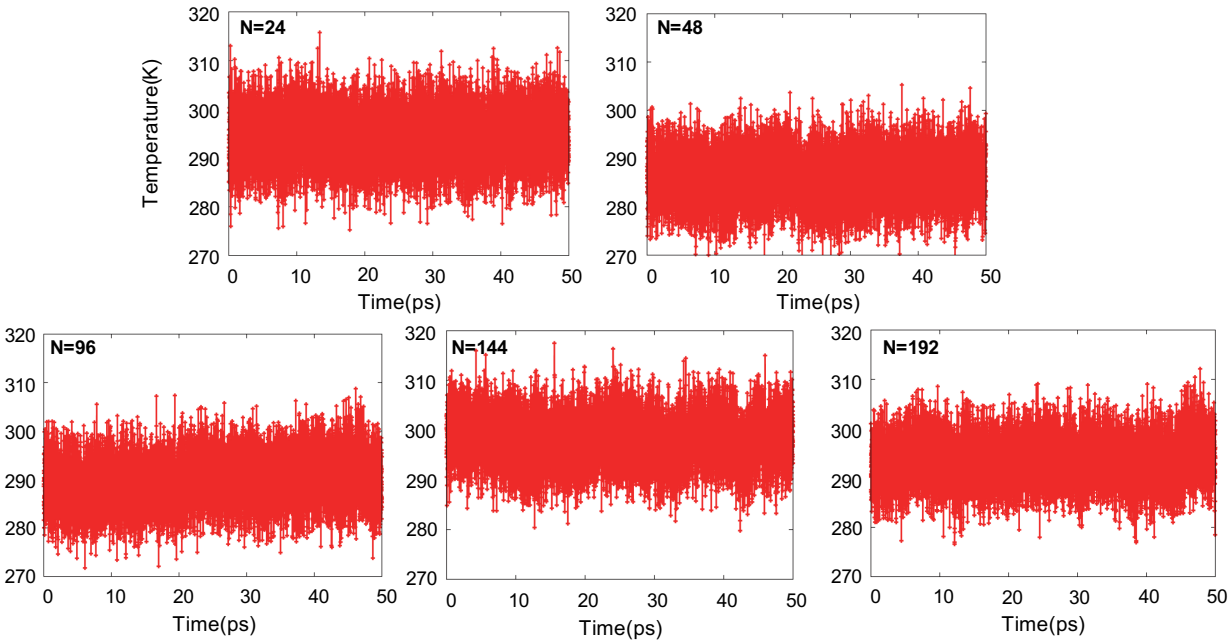

Figure S17: Simulation Temperature of the 6th NVE trajectory for different water content in the $Cu_3(HHTP)_2$ 2D MOF.

References

(1) Hmadeh, M. et al. New porous crystals of extended metal-catecholates. *Chem. Mater.* **2012**, *24*, 3511–3513.

(2) Perdew, J. P.; Burke, K.; Ernzerhoff, M. Erratum: Generalized gradient approximation made simple. *Phys. Rev. Lett.* **1996**, *78*, 1396–1396.

(3) Grimme, S.; Antony, J.; Ehrlich, S.; Krieg, H. A consistent and accurate ab initio parametrization of density functional dispersion correction (DFT-D) for the 94 elements H-Pu. *J. Chem. Phys.* **2010**, *132*, 154104.

(4) Hutter, J.; Iannuzzi, M.; Schiffmann, F.; VandeVondele, J. cp2k: atomistic simulations of condensed matter systems. *WIREs Computational Molecular Science* **2014**, *4*, 15–25.

(5) Wang, J.; Wolf, R. M.; Caldwell, J. W.; Kollman, P. A.; Case, D. A. Development and testing of a general amber force field. *J. Computat. Chem.* **2004**, *25*, 1157–1174.

(6) Goldberg, D. *Genetic Algorithms in Search, Optimization and Machine Learning,*; Addison-Wesley, 1989.

(7) Mardirossian, N.; Head-Gordon, M. ωB97M-V: A combinatorially optimized, range-separated hybrid, meta-GGA density functional with VV10 nonlocal correlation. *J. Chem. Phys.* **2016**, *144*, 214110.

(8) Shao, Y.; Gan, Z.; Epifanovsky, E.; Gilbert, A. T.; Wormit, M.; Kussmann, J.; Lange, A. W.; Behn, A.; Deng, J.; Feng, X., et al. Advances in molecular quantum chemistry contained in the Q-Chem 4 program package. *Mol. Phys.* **2015**, *113*, 184–215.

(9) Breneman, C. M.; Wiberg, K. B. Determining atom-centered monopoles from molecular electrostatic potentials. The need for high sampling density in formamide conformational analysis. *J. Comput. Chem.* **1990**, *11*, 361–373.

(10) Rappe, A. K.; Casewit, C. J.; Colwell, K. S.; III, W. A. G.; Skiff, W. M. UFF, a full periodic table force field for molecular mechanics and molecular dynamics simulations. *J. Am. Chem. Soc.* **1992**, *114*, 10024–10035.

(11) Rieth, A. J.; Hunter, K. M.; Dincă, M.; Paesani, F. Hydrogen bonding structure of confined water templated by a metal-organic framework with open metal sites. *Nat. Commun.* **2019**, *10*, 4771.

(12) Mendecki, L.; Mirica, K. Conductive metal–organic frameworks as ion-to-electron transducers in potentiometric sensors. *ACS Appl. Mater. Interfaces* **2018**, *10*, 19248–19257.

(13) Day, R. W.; Bediako, D. K.; Rezaee, M.; Parent, L. R.; Skorupakii, G.; Arguilla, M. Q.; Hendon, C. H.; Stassen, I.; Gianneschi, N. C.; Kim, P.; Dincă, M. Single Crystals of Electrically Conductive Two-Dimensional Metal-Organic Frameworks: Structural and Electrical Transport Properties. *ACS Cent. Sci.* **2019**, *5*, 1959–1964.

(14) Frisch, M. J., et al. Gaussian 16 Revision C.01. Gaussian Inc.: Wallingford CT, 2016.

(15) Zhao, Y.; Truhlar, D. G. A new local density functional for main-group thermochemistry, transition metal bonding, thermochemical kinetics, and noncovalent interactions. *J. Chem. Phys.* **2006**, *125*, 194101.

(16) Weigend, F. Accurate Coulomb-fitting basis sets for H to Rn. *Phys. Chem. Chem. Phys.* **2006**, *8*, 1057–1065.

(17) Cramer, C. J. *Essentials of Computational Chemistry: Theories and Models*, 2nd ed.; John Wiley & Sons: Chichester, 2004.

(18) Smith, T., W.; Forester DL POLY 2.0: A general-purpose parallel molecular dynamics simulation package. *J. Mol. Graph.* **1996**, *14*, 136–141.

(19) Martínez, L.; Andrade, R.; Birgin, E. G.; Martínez, J. M. PACKMOL: A package for

building initial configurations for molecular dynamics simulations. *J. Comput. Chem.* **2009**, *30*, 2157–2164.

(20) Tuckerman, M. E. *Statistical mechanics: Theory and molecular simulation*; (Oxford University Press, 2010.

(21) Leach, A. R. *Molecular modeling: Principles and applications*; Pearson Prentice Hall, 2001.

(22) Abascal, C., J. L. F.; Vega A general purpose model for the condensed phases of water: TIP4P/2005. *J. Chem. Phys.* **2005**, *123*, 234505.

(23) Habershon, T. E. M. D. E., S.; Markland Competing quantum effects in the dynamics of a flexible water model. *J. Chem. Phys.* **2009**, *131*, 024501.

(24) Babin, V. http://deleramentum.net/codes/ttm/.

Structure: CAT

Charge: 0 **Multiplicity:** 1

C	1.81600900	0.72567800	-0.00004100
C	0.61862600	1.41064200	0.00012100
H	0.59762700	2.50735900	0.00012900
C	-0.67285200	0.75654600	0.00003100
O	-1.74245700	1.39955500	-0.00008700
C	1.81600400	-0.72568100	-0.00006000
C	0.61862000	-1.41064300	0.00006900
H	0.59762800	-2.50736100	0.00002700
O	-1.74246200	-1.39954900	-0.00001300
C	-0.67285600	-0.75654500	0.00003500
H	2.77140100	1.26321100	-0.00012500
H	2.77139200	-1.26322100	-0.00017100

Structure: Co-CAT

Charge: +1 **Multiplicity:** 4

C	-2.81636300	-0.72574100	0.00006800
C	-1.63902600	-1.44372500	-0.00000700
H	-1.61976600	-2.53400000	-0.00001800
C	-0.42668700	-0.72978500	-0.00007000
O	0.75478500	-1.28558700	-0.00013000
C	-2.81635800	0.72575600	0.00007000
C	-1.63901500	1.44372900	-0.00001000
H	-1.61972400	2.53400400	-0.00002200
O	0.75479500	1.28556900	-0.00012700
C	-0.42668500	0.72977700	-0.00007100
H	-3.77409800	-1.24926200	0.00012000
H	-3.77409200	1.24928000	0.00011600
Co	2.12206800	0.00000200	0.00007300

Structure: Co-2CAT

Charge: 0 **Multiplicity:** 2

C	4.93550000	0.72786300	-0.00117000
O	-1.36007500	-1.26563600	0.01406200
C	3.75508200	1.43830400	-0.00344400
H	3.73028600	2.52927000	-0.00813300
C	2.53792800	0.72263200	-0.00552200
C	-2.54030300	-0.72087600	-0.00518300
O	1.36183900	1.26811300	-0.02207500

C	4.93753900	-0.72349600	0.00213300
C	3.75822500	-1.43620900	0.00389800
H	3.73554200	-2.52724000	0.00857000
C	-4.93589200	0.72737500	0.01529100
O	1.36401100	-1.27050500	0.02157100
C	-3.75379000	1.43728700	0.02686700
H	-3.72844700	2.52818400	0.04335300
C	-2.53916400	0.72048300	0.00510000
C	2.53932400	-0.72306500	0.00544200
O	-1.35817800	1.26336900	-0.01465100
C	-4.93730400	-0.72325400	-0.01428700
C	-3.75639800	-1.43535300	-0.02638600
H	-3.73317000	-2.52630500	-0.04290200
Co	-0.00259800	-0.00182300	-0.00042000
H	-5.89508400	-1.24744400	-0.02322000
H	-5.89272300	1.25331400	0.02463800
H	5.89264400	1.25340700	-0.00286700
H	5.89584600	-1.24682600	0.00422800

Structure: Co-2CAT-H_2O

Charge: 0 **Multiplicity:** 2

C	4.92715600	0.72851000	-0.33698300
O	-1.38372700	-1.27939800	-0.13037900
C	3.74511700	1.43469900	-0.25466600
H	3.71744400	2.52603400	-0.26850200
C	2.53286200	0.72076100	-0.15452300
C	-2.54844700	-0.72574900	-0.16829000
O	1.35796800	1.27486300	-0.07191600
C	4.92936700	-0.72277000	-0.32157800
C	3.74955700	-1.43151000	-0.22963200
H	3.72580500	-2.52301700	-0.22500000
C	-4.94400800	0.72767800	-0.26945700
O	1.36082500	-1.27643700	-0.06240100
C	-3.76784600	1.43837000	-0.20804000
H	-3.74459800	2.52944400	-0.19902500
C	-2.54749700	0.72569500	-0.15690900
C	2.53465400	-0.72008900	-0.14572200
O	-1.38227600	1.27772200	-0.11610100
C	-4.94547600	-0.72314500	-0.28693500
C	-3.76967000	-1.43591600	-0.23772000
H	-3.74725000	-2.52699100	-0.25093100
Co	-0.00858300	-0.00163000	-0.00914300
H	-5.90329400	-1.24524200	-0.33830800
H	-5.90122200	1.25211800	-0.30798900

H	5.88015600	1.25583100	-0.41566700
H	5.88412400	-1.24850300	-0.38913500
O	0.02573600	-0.00491500	2.18044300
H	0.56027000	-0.77014900	2.43104200
H	0.55747100	0.76059500	2.43596800

Structure: Co-2CAT-2H_2O

Charge: 0 **Multiplicity:** 2

C	4.93502100	0.72755300	-0.06712500
O	-1.35660300	-1.30217700	-0.12528600
C	3.74317400	1.42630600	-0.01566800
H	3.71160600	2.51773600	-0.02630800
C	2.53104800	0.71720300	0.04881000
C	-2.53238600	-0.71724700	-0.05677600
O	1.35487500	1.30075400	0.11928700
C	4.93730700	-0.72372200	-0.05071400
C	3.74678400	-1.42435700	0.00966500
H	3.71786800	-2.51590100	0.01763000
C	-4.93532800	0.72722800	0.06472600
O	1.35685700	-1.30226700	0.12617700
C	-3.74340300	1.42616500	0.01465100
H	-3.71194900	2.51760000	0.02539200
C	-2.53113100	0.71720100	-0.04859000
C	2.53250100	-0.71728900	0.05680000
O	-1.35480300	1.30079000	-0.11792900
C	-4.93713800	-0.72361200	0.04829500
C	-3.74659100	-1.42434100	-0.01087000
H	-3.71774700	-2.51588000	-0.01887200
Co	-0.00001900	-0.00142100	0.00070900
H	-5.89000700	-1.25511100	0.08997700
H	-5.88690100	1.25998400	0.11820800
H	5.88647400	1.26042700	-0.12164600
H	5.89023500	-1.25499900	-0.09342200
O	-0.09054100	-0.00154100	1.96502000
H	0.45141300	-0.77415900	2.19978200
H	0.44506200	0.77504500	2.20095700
O	0.09054100	-0.00110400	-1.96388600
H	-0.45150500	-0.77383700	-2.19816600
H	-0.44580100	0.77526700	-2.19896600

Structure: Co-CAT-H_2O

Charge: +1 **Multiplicity:** 3

O	-0.16795600	-1.40199000	0.00009000
C	0.92919200	-0.74425200	0.00016800
O	-3.46846000	0.59445500	-0.00050200
C	3.18593100	0.92924000	0.00031000
C	1.96514700	1.54687200	0.00016900
H	1.85904300	2.63237400	0.00011300
C	0.79008800	0.73897700	0.00009100
O	-0.39376400	1.18583400	-0.00002400
C	3.31437900	-0.51599800	0.00037800
C	2.21601500	-1.33815200	0.00031500
H	2.29935000	-2.42568500	0.00037100
Co	-1.73475600	-0.34586500	-0.00019000
H	4.31728900	-0.94749400	0.00049200
H	4.09855800	1.52873200	0.00036200
H	-4.37753600	0.26171700	-0.00082000
H	-3.52135900	1.56221600	-0.00048100

Structure: Co-CAT-2H_2O

Charge: +1 **Multiplicity:** 3

O	0.06288000	1.21624900	-0.46380400
C	-1.08827800	0.69789800	-0.24322400
O	2.67815000	-1.49641200	-0.72593100
C	-3.49134300	-0.69003300	0.22394100
O	2.67814000	1.49644000	0.72585900
C	-2.32060800	-1.37116900	0.44554300
H	-2.30651100	-2.40536300	0.79248400
C	-1.08828400	-0.69788900	0.24324500
O	0.06287000	-1.21623300	0.46386300
C	-3.49133800	0.69003000	-0.22398400
C	-2.32060300	1.37117300	-0.44555400
H	-2.30651100	2.40536800	-0.79249400
Co	1.52330100	-0.00001700	0.00001900
H	-4.45076300	1.18404100	-0.38946200
H	-4.45077100	-1.18404700	0.38939200
H	3.37882700	-1.50639300	-1.39189800
H	2.28711200	-2.38252300	-0.71564900
H	3.37881800	1.50642700	1.39182400
H	2.28707200	2.38253800	0.71559800

Structure: Co-CAT-3H_2O

Charge: +1 **Multiplicity:** 3

O	0.22069800	-1.37339400	0.12164600
C	1.31916600	-0.72708700	0.07109800

O	-2.67974900	1.62412800	-0.10353800
C	3.63620500	0.88576100	-0.06096500
O	-2.14358300	-0.50630900	1.79861600
C	2.41508800	1.51246500	-0.15380500
H	2.32981400	2.59358900	-0.27519400
C	1.23226400	0.73890900	-0.09336000
O	0.04530300	1.23922200	-0.17923000
C	3.72967100	-0.55335300	0.09848500
C	2.60462500	-1.33483700	0.16105600
H	2.65898500	-2.41819000	0.28138300
Co	-1.36685100	-0.06380800	-0.02941700
H	4.71933300	-1.00898100	0.16859500
H	4.55735100	1.46993300	-0.10690700
O	-2.03722000	-1.24101500	-1.55460500
H	-1.48255000	-2.01131200	-1.74398500
H	-2.66330500	-1.15071400	-2.28343800
H	-3.51584900	1.82580200	-0.54129700
H	-2.12108400	2.40502900	-0.23150000
H	-2.71731700	0.07242600	2.31755700
H	-1.72612300	-1.12698000	2.41087000

Structure: Co-CAT-4H_2O

Charge: +1 **Multiplicity:** 3

O	0.34084800	-1.34190700	0.23069000
C	1.46163900	-0.73667200	0.14229200
O	-2.58388400	1.67171700	-0.18917800
C	3.84657100	0.76816600	-0.09725600
O	-2.97944700	-1.21301700	0.17258900
C	2.65080200	1.43103700	-0.24435100
H	2.60874300	2.50283900	-0.44691400
C	1.43146400	0.71624000	-0.13180500
O	0.27415200	1.26497800	-0.25481700
C	3.88205700	-0.65708100	0.17222000
C	2.72347500	-1.38329400	0.28747400
H	2.73331000	-2.45589100	0.49055800
Co	-1.22483800	0.01781600	-0.02871000
H	4.85163300	-1.14668800	0.28309000
H	4.78993600	1.31123200	-0.18186900
O	-1.28058900	-0.77355000	-2.01138800
H	-0.51085900	-1.34862200	-2.13149800
H	-1.36246200	-0.27030000	-2.83186800
O	-1.47109400	0.20586300	2.06833000
H	-0.73521100	-0.08055800	2.62661800
H	-1.74672100	1.06692000	2.41080400

H	-3.51079400	1.62201100	-0.45383800
H	-2.24848900	2.51198200	-0.52812100
H	-3.13540400	-1.56475900	1.05932900
H	-3.03898500	-1.97225900	-0.42237800

Structure: Cu-CAT

Charge: +1 **Multiplicity:** 1

C	2.89375900	0.73100500	0.01311600
C	1.75022500	1.46522100	0.02636900
H	1.74820400	2.55588100	0.03909200
C	0.49109400	0.77134800	-0.00143300
O	-0.61608900	1.32228600	-0.03866300
C	2.89385300	-0.73080100	-0.01273800
C	1.75042200	-1.46516000	-0.02638000
H	1.74854800	-2.55582000	-0.03909900
O	-0.61593600	-1.32252800	0.03788600
C	0.49117500	-0.77144900	0.00106800
Cu	-2.17197400	0.00001900	0.00019000
H	3.86169100	1.23744300	0.01832400
H	3.86185200	-1.23711600	-0.01760900

Structure: Cu-2CAT

Charge: 0 **Multiplicity:** 2

C	-5.07512800	-0.60752400	-0.01653300
O	1.43072000	1.22345300	-0.32314000
C	-3.93924000	-1.38294100	-0.02135400
H	-3.98037200	-2.47302400	-0.06508500
C	-2.66547300	-0.73941300	-0.08536900
C	2.58755700	0.72348900	-0.12253800
O	-1.56807400	-1.30157500	-0.36675100
C	-4.99051500	0.85187000	-0.04244300
C	-3.78272800	1.50147800	0.01420300
H	-3.70798800	2.58958700	0.05721400
C	5.08430600	-0.60858100	0.02238000
O	-1.45696100	1.17247400	0.45536000
C	3.93712000	-1.36905600	0.07461600
H	3.96996000	-2.45789800	0.15158200
C	2.66012100	-0.73279900	0.07991000
C	-2.59350300	0.72437800	0.13330500
O	1.55308300	-1.34278600	0.26470700
C	4.99982200	0.84827900	-0.01924700
C	3.78659000	1.48845000	-0.09460200

H	3.71000400	2.57485900	-0.17008100
Cu	0.00941100	-0.10776700	0.01138700
H	6.06732000	-1.08292600	0.04878900
H	5.92671700	1.42639800	-0.02559100
H	-6.06181400	-1.07453300	-0.04108200
H	-5.92045500	1.42448400	-0.06133000

Structure: Cu-2CAT-H_2O

Charge: 0 **Multiplicity:** 2

C	-5.07318700	-0.64799500	-0.21549100
O	1.41926100	1.20422100	-0.31020300
C	-3.91863500	-1.39947100	-0.14273200
H	-3.94280400	-2.49057300	-0.10156900
C	-2.64719000	-0.75705600	-0.14587800
C	2.58703800	0.70013100	-0.23468300
O	-1.52482300	-1.37912300	-0.13717200
C	-4.99167600	0.81003400	-0.28661600
C	-3.78062100	1.45965100	-0.27656900
H	-3.70889800	2.54801700	-0.32416400
C	5.08627800	-0.62507600	-0.16590600
O	-1.41714400	1.23491200	-0.09548600
C	3.94710100	-1.39441300	-0.10908200
H	3.98793900	-2.48302800	-0.03696100
C	2.66599700	-0.76724800	-0.11329700
C	-2.58231100	0.70803100	-0.17645900
O	1.55997600	-1.39165500	-0.01311700
C	4.99860800	0.82955400	-0.25351900
C	3.78320600	1.46747100	-0.28198500
H	3.69986500	2.55333500	-0.35551600
Cu	0.01030100	-0.14508600	-0.06792900
H	6.07229300	-1.09333200	-0.14246900
H	5.92438400	1.40720100	-0.29939500
H	-6.05314100	-1.12836900	-0.22869700
H	-5.92041400	1.38216100	-0.34523100
O	0.00049700	0.34584900	2.24769300
H	-0.74965500	-0.12672500	2.62848400
H	-0.35809100	1.22348600	2.05504300

Structure: Cu-2CAT-$2H_2O$

Charge: 0 **Multiplicity:** 2

C	5.07713900	-0.63897000	0.07583400
O	-1.41932400	1.22873100	0.06679400

C	3.93196800	-1.39931600	0.04040500
H	3.96248900	-2.49078100	0.05883900
C	2.65430800	-0.76825000	-0.01722500
C	-2.58588600	0.69837600	0.02645700
O	1.55075300	-1.41260100	-0.06937300
C	4.99324200	0.82046400	0.05213100
C	3.78061400	1.46018100	-0.00656900
H	3.70204900	2.54912200	-0.02251800
C	-5.08187000	-0.63711900	-0.03160500
O	1.41891900	1.23092300	-0.10510400
C	-3.93657600	-1.39824000	0.00457300
H	-3.96803700	-2.48980400	0.00807900
C	-2.65964900	-0.76583100	0.03403100
C	2.58146900	0.70007300	-0.04001600
O	-1.55269100	-1.40935800	0.08447500
C	-4.99675300	0.82028500	-0.03771400
C	-3.78278500	1.46036300	-0.00778600
H	-3.70307000	2.54927800	-0.01494900
Cu	-0.00477400	-0.16959000	-0.00914800
H	-6.06511000	-1.11100800	-0.05878500
H	-5.92321300	1.39838700	-0.06956200
H	6.05976200	-1.11244600	0.12475200
H	5.92005900	1.39800900	0.08437500
O	0.06271100	0.23829200	2.35319200
H	-0.73949900	-0.19941900	2.66300300
H	-0.22890100	1.14307200	2.17506300
O	-0.03240600	0.17422000	-2.37445600
H	0.75614700	-0.30317600	-2.65998400
H	0.29074700	1.07312100	-2.22235000

Structure: Cu-CAT-H_2O

Charge: +1 **Multiplicity:** 1

C	3.34687200	0.74667700	0.04885800
C	2.19801600	1.47400100	0.06662900
H	2.19061300	2.56432600	0.09662500
C	0.94538200	0.77140800	-0.00897900
O	-0.16853200	1.30226100	-0.10294100
C	3.35322800	-0.71423200	-0.00815700
C	2.21094500	-1.45162600	-0.05255300
H	2.21354600	-2.54196800	-0.08237000
O	-0.15922400	-1.30230600	0.05249800
C	0.95336600	-0.75903900	-0.00847000
O	-3.67900300	0.07564800	0.04308600
Cu	-1.74234100	-0.04510500	-0.01400800

H	4.31235800	1.25707000	0.07118300
H	4.32296100	-1.21706100	-0.00792700
H	-4.29513000	-0.62980600	0.28122700
H	-4.20925500	0.86753100	-0.11761100

Structure: Cu-CAT-2H_2O

Charge: +1 **Multiplicity:** 1

C	-3.56304400	-0.72774900	-0.06698200
O	2.82607000	1.46961800	-0.40560600
C	-2.40728000	-1.45191600	-0.13102900
H	-2.40097900	-2.53420000	-0.26780800
C	-1.16678600	-0.73999800	-0.14445600
O	-0.05478800	-1.23398700	-0.43987700
C	-3.56292100	0.72807700	0.06761700
C	-2.40704000	1.45209800	0.13121200
H	-2.40054600	2.53438200	0.26797800
O	-0.05444900	1.23385500	0.43910600
C	-1.16663700	0.74001900	0.14414900
O	2.82588000	-1.46935800	0.40665300
Cu	1.48794900	-0.00021300	-0.00032000
H	-4.52798500	-1.23440100	-0.13603300
H	-4.52776900	1.23485600	0.13704500
H	3.49726700	-1.44090600	1.10082900
H	2.50607900	-2.38135500	0.37973500
H	3.49788900	1.44203800	-1.09942000
H	2.50607500	2.38154800	-0.37831400

Structure: Cu-CAT-3H_2O

Charge: +1 **Multiplicity:** 1

C	-3.83138200	-0.63382100	0.13759600
O	2.73839600	0.82060200	-1.23793500
C	-2.70315700	-1.40124100	0.20566000
H	-2.73975400	-2.48619300	0.31466900
C	-1.43994200	-0.76463100	-0.00440900
O	-0.35829000	-1.36044700	-0.21517300
C	-3.77471600	0.81410000	-0.05706900
C	-2.58957400	1.48190200	-0.18572000
H	-2.53892900	2.56634900	-0.29481100
O	-0.23709100	1.23540600	0.11739200
C	-1.37609500	0.73818800	-0.04684900
O	2.53457300	-1.70959500	0.28651800
Cu	1.25819200	-0.13195100	-0.16086500

H	-4.81513200	-1.10238000	0.21020900
H	-4.71721600	1.36522400	-0.07849400
O	2.41841000	1.15471300	1.40888600
H	2.93412500	0.75857600	2.12342400
H	1.84862800	1.80303700	1.84397100
H	3.28568200	-1.81309900	-0.31357900
H	2.10187700	-2.57444800	0.30588400
H	3.08054900	1.44330800	-0.57561800
H	2.59379800	1.33378200	-2.04332800

Structure: Cu-CAT-4H_2O

Charge: +1 **Multiplicity:** 1

C	4.02855600	-0.48168500	-0.19355100
O	-1.99410100	2.59809700	-0.26728900
C	2.96676900	-1.33809400	-0.26599200
H	3.09022800	-2.41261800	-0.40883600
C	1.65732500	-0.81882700	-0.01746000
O	0.63998500	-1.51974600	0.19878100
C	3.84914100	0.94837100	0.05172000
C	2.61122300	1.50549500	0.22216300
H	2.47467000	2.57738600	0.37405300
O	0.27689400	1.06237900	-0.03332100
C	1.46605700	0.66690400	0.07911600
O	-2.48841900	-2.01872000	-0.06609200
Cu	-1.08042000	-0.51342700	0.24528800
H	5.04696500	-0.86099300	-0.29869600
H	4.73944300	1.58011800	0.07886700
O	-2.35960400	0.52730100	1.41902000
H	-3.23826000	0.14132300	1.52585600
H	-2.48201500	1.42151500	1.03426000
O	-2.22754100	0.20636400	-1.65100600
H	-1.81700700	0.23820700	-2.52371800
H	-2.35432800	1.14542100	-1.41109600
H	-2.90738000	-1.78568000	-0.90837700
H	-2.25810900	-2.95511700	-0.12407100
H	-2.18848900	3.54171600	-0.31985400
H	-1.02567000	2.51971100	-0.18846500